Stereolithography of (meth)acrylate-based photocurable resin: Thermal and mechanical properties

Nader Zirak[1,3] **Mohammadali Shirinbayan**[1,3] **Khaled Benfriha**[2]
Michael Deligant[3] **Abbas Tcharkhtchi**[1]

[1]Arts Et Metiers Institute of Technology, CNRS, CNAM, PIMM, HESAM University, Paris, France

[2]Arts Et Metiers Institute of Technology, CNAM, LCPI, HESAM University, Paris, France

[3]Arts Et Métiers Institute of Technology, CNAM, LIFSE, HESAM University, Paris, France

Correspondence
Nader Zirak, Arts et Metiers Institute of Technology, CNRS, CNAM, PIMM, HESAM University, 75013 Paris, France.
Email: nader.zirak@ensam.eu

Abstract

Additive manufacturing (AM) has attracted a lot of attention in the industry and studies due to the ability to fabricate parts in different sizes and shapes along with economic costs. Among the different three-dimensional (3D) printing methods, stereolithography (SLA) is becoming an important method. The objective of this work is to investigate the effect of different sub-build orientations of an acrylate-based 3D printing SLA rapid-prototyping photosensitive resin concerning UV and thermal post-curing on the thermal and mechanical properties. Key role of polymerization as a determining factor in the final mechanical and thermal properties was shown. The results indicate turning the mechanical properties of cured resin by different sub-build orientations. Furthermore, post-curing process was performed in order to complete the curing of unreacted monomers. The results show the important effect of thermal post-curing on the mechanical properties. In addition, a polymerization up to 98% for thermal curing at 80°C was achieved. In addition, the maximum tensile strength for the maximum amount of polymerization was for sub-building orientation of 45°, 0°, and 90°.

KEYWORDS

crosslinking, differential scanning calorimetry, manufacturing, thermogravimetric analysis

1 | INTRODUCTION

Three-dimensional (3D)-printing technology has been one of the most important processes that have undergone changes and have attracted a lot of attention. Generally, in this method, fabrication of the part completed by placing one layer of material on top of the other.[1,2] Among the various methods in 3D printing, stereolithography (SLA) due to the high accuracy, smooth surface finishing, the ability to produce transparent objects, and the incorporation of fine details, for example, compared to the fused deposition modeling has been the center of attention of studies.[3–5] In this method scanning the resin surface by a laser, which is programmed before, can cause polymerization or cross-linking and leads to the fabrication of the parts. This process consists of layer-by-layer polymerization of the photosensitive resin.[6] Some of the applications of this method can be addressed to the automobile, electric, biomedical, and aerospace industries.[7–9]

Parameters such as laser power distribution and scanning speed during construction, resin characteristics (such as monomers, oligomers, and curing agent compositions) can play a decisive role the maximum density of cross-linking and consequently final properties.[8,10] Generally, acrylates, vinyl ethers, and epoxides have been among the types of multifunctional monomers which were used for laser-induced polymerization.[11–13] In the different types of multifunctional resins producing, the

https://doi.org/10.1002/app.52248

mechanism of polymerization occurs by reaction of the acrylate group and an epoxy group through a radical and cationic mechanism, respectively.[14,15]

According to the applications mentioned for this method, having suitable properties play an important role in the efficiency of the parts produced by this process. For this purpose, the polymerization of the polymer has played the most important role in determining the final behavior of the parts.[16,17] After fabrication, the sample is quite hard, but an increase in the polymerization by post-curing apparatus is an important step to increasing the cross-link density and removing residual resin.[18] In most cases, produced parts can be cured by the use of high-intensity ultraviolet (UV) light and temperature.[19,20]

Resin composition and production parameters have a determining role in the degree of cure. Uzcategui et al.[21] studied the effect of processing parameters on mechanical properties and developing a dual-cure system with an ability of 100% conversion on a multifunctional acrylate-based resin. For post processing, removing the unreacted monomer by a solvent was the first post processing. Considering the plasticization effect of unreacted monomer, they showed a key importance role of using a solvent for removing this monomer for improving mechanical behavior. In addition, thermal post curing was significantly has been increased the modulus of samples. This increase was from 7 to 15 MPa through thermal cure. However, studies have shown that the degree of cure in the parts fabricated without post-curing was about 80%, and subsequent treatment operations were necessary to achieve more than 90% curing. In a study by Fuh et al.[10] 94% degree of cure by using the UV light for 120 s was achieved. On the other hand, the use of temperature has been another method of curing, which used in many studies. In this method, using the sample in chamber at a constant temperature for a certain period of time leads to an increase in the amount of cross-links density. In general, depending on the composition, the temperature range can consist of 40–140°C. Also, the curing time period has been in the range of several min to several hours. Hague et al.[19] studied the effect of UV and thermal post-curing of the Acura SI40 and SL 7560 resins. Their showed the important role of thermal post-curing cycle on mechanical properties. Post curing was performed by using the UV and thermal condition in the time range of 90 and 120 min, respectively. However, optimization and using the best condition during post-curing by evaluating various parameters, including changes in the time and temperature have been studied in many researches.[14,22,23] It is worth noting that the effect of temperature and time on creating the residual stresses in the end parts should be considered. Therefore, clarifying the relationship between mechanical properties and post-curing from the parts by considering the properties of the resin plays an important role to achieve the set of the best parameters.[24,25]

Among the resins, acrylate-based resins due to their high hydrophobicity, high accuracy, and low cost have attracted the attention of many studies[26,27] which using a broad range of multifunctional acrylate in the system can lead to the excellent performance of the produced parts.[28] In this study, acrylate-based resin was considered for the fabrication of the parts. Due to the importance of polymerization of the samples, the post-curing process by using UV with and without heating was used. Also, due to the importance of anisotropy in the produced parts, this parameter was evaluated by fabrication of samples in different sub-build orientations. Finally, the physico–chemical, thermal, and mechanical properties of the parts were evaluated by Fourier-transform infrared spectroscopy (FTIR), differential scanning calorimetry (DSC), thermogravimetric analysis (TGA), DMA, and tensile test analysis. The results showed a key role of post-curing on the final properties. In addition, according to the results, the maximum tensile strength was ranked as follows: $90^\circ < 0^\circ < 45^\circ$.

2 | MATERIALS AND METHODS

2.1 | Materials

A photoresist, Black Resin (product code: FLGPBK04) from Formlabs (Berlin, Germany), was used in this study. According to the datasheet, the resin was consisting of urethane dimethacrylate (UDMA) diluted with the corresponding methacrylate monomers, and bis(2,-4,6-trimethylbenzoyl) phenylphosphine oxide as a photoinitiator. Ethanol with 100% purity was used to wash the samples after printing.

2.2 | Sample preparation

Formlabs Form 3-printer machine was used to fabrication the samples. Then, by the Preform software, the tensile samples (ISO 3167 type B[29]) were prepared in stl.file format for printing. The different orientations in 0°, 45°, and 90° (with respect to the x direction) with a automatically support were prepared. The thickness of the layers and printing speed were 100 microns and 20 mm/s, respectively. Figure 1 shows the schematic of printed samples in different sub-build orientations. Immediately washing was performed in an alcohol bath for 30 min after printing. Then the support was separated from the samples and green samples were produced. The green

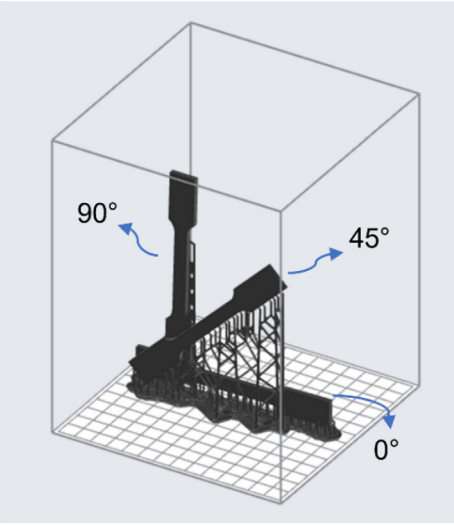

FIGURE 1 Schematic of printed samples in different sub-build orientations [Color figure can be viewed at wileyonlinelibrary.com]

samples in different directions for the post-curing process were collected. The post-curing was applied for 30 min with two posturing mechanisms: using UV without heating and UV with the heating in the temperature range of 40, 50, 60, and 80°C.

2.3 | FTIR analysis

FTIR was used to analyze the residual percentage of unpolymerized of UDMA in the samples. A FTIR spectrometer (potassium bromide [KBr] powder transmission) was used for the tests and the wavenumber was in the range of 4000–400 cm^{-1}.

2.4 | DSC analysis

DSC was carried out (Q1000 V9.0 Build 275 DSC, TA instrument) to investigate the degree of post-curing of the samples. In this regard, approximately 8 g of each sample 0°-printed was removed, and then the thermogram heating was carried out from 80 up to 210°C. The heating rate and nitrogen gas flow were 10°C/min and 50 ml/min, respectively.

2.5 | TGA analysis

Thermal stability of samples was analyzed by TGA, using a METTLER TOLEDO 822e instrument (Ohio, U.S.). Regarding, samples were weighted in the range of 9–10 mg. The test was performed at a temperature from 25 to 800°C by a heating rate of 10°C/min under nitrogen flow of 50 ml/min.

2.6 | DMTA analysis

Dynamic mechanical thermal analysis (DMTA) in flexion mode were performed by the device Dynamic Mechanical Analyzer type Q800 V21. Regarding, rectangular samples were printed at 0° in dimensions of $35 \times 10 \times 4\ mm^3$. The condition of the test was set for temperature in the range of 25 up to 250°C with a heating rate of 3.00°C/min at multi-frequency of 1, 3, 10, and 30 Hz. Finally, storage modulus (E′), loss modulus (E") and loss tangent or tan δ (E"/E′) were measured against the temperature.

2.7 | Mechanical characterization

For analyzing the mechanical properties quasistatic tensile tests were performed by using the MTS 830 hydraulic machine with a loading cell of 10 kN at a constant ramp speed of 5 mm/min. At least four repetitions were performed for each tensile test, and the average of results was finally reported.

3 | RESULTS AND DISCUSSION

3.1 | Effect of post-curing on polymerization

The effect of post-curing on the polymerization of the samples was studied by using the FTIR and DSC in this study. Regarding, from the FTIR results, absorption changes in the functional groups were investigated. Figure 2 shows the FTIR results related to the green, UV, and UV with heat curing at different temperatures in the range of 40–80°C for 0°-printed samples. The absorption bands related to the methacrylate function, amide II vibration, and the C—O—C have appeared at the peaks of 1637, 1535, and 1100–1245 cm^{-1}, respectively.[30,31] The absorption peak in 1701 cm^{-1} is corresponding to the C═O bond for UDMA.[32]

Two absorption peaks of C═C at 1630 cm^{-1} and amide II at 1532 cm^{-1} (I_{1630}/I_{1532} cm^{-1}) were considered as an index for the calculation of residual unpolymerized monomers.[30,33] The ratio obtained for the green sample was considered to control which ratio shows the 100% residual of unpolymerized monomers. Consequently, residual unpolymerized monomers for post-cured samples according to the control ratio were calculated. According to the intensity ratio, the percentage of

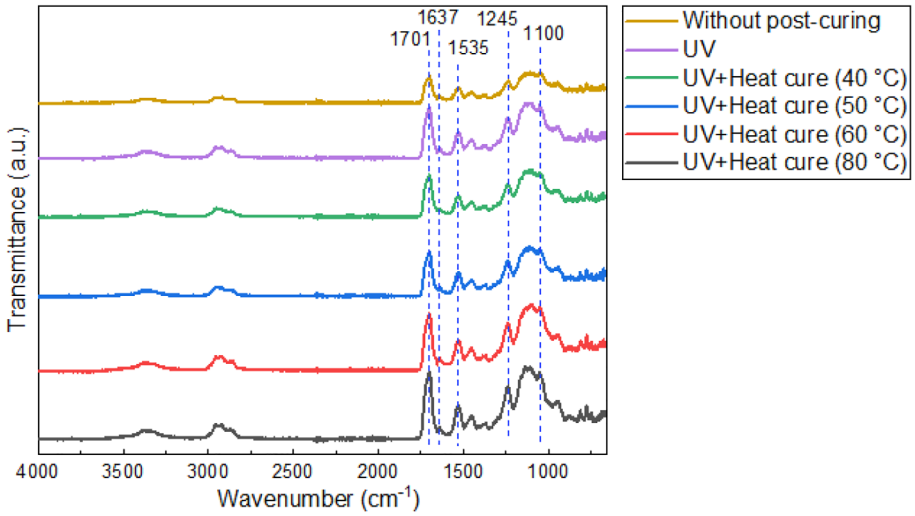

FIGURE 2 FTIR spectrum of samples in green and post-cured condition. FTIR, Fourier-transform infrared spectroscopy [Color figure can be viewed at wileyonlinelibrary.com]

residual UDMA for UV, UV with heat 40°C, UV with heat 50°C, UV with heat 60°C, and UV with heat 80°C post-cured samples were 83.77%, 82.36%, 79.36%, 76.01%, and 67.37%, respectively.

Curing the resin in SLA can be divided into two mechanisms of photocuring and thermal curing.[34] Photocuring mechanism in (meth)acrylate-based resin performs by the radical system which is consists of radical generation, initiation, and propagation of radical. For the first step of this mechanism, radical generation occurs by converting photolytic energy into a reaction for the initiation of polymerization.[12] On the other hand, thermal curing is another mechanism that polymerization is happening by photo initiators with temperature (all of the SLA resins have photo initiators for curing with temperature).[23] For investigation of curing mechanisms, studies have been analyzed two peaks of C═C bands at 810 and 1632 cm^{-1} that are related to the acrylate group.[35,36] Changes in the absorption of these peaks represent the polymerization of monomers during the crosslinking reaction.[37–39] Figure 3 shows the ratio of I_{1701}/I_{810} cm^{-1} against the temperature. The Figure showed the linear relation with a threshold in the 50°C ($R > 0.98$). First, the polymer main chain crosslinking reaction is dominant. On the other hand, It can be mentioned that the second slop is related to the side photochemical reactions of the macromolecular chains end groups. According to the temperature range used in post-curing, it can be said that the mechanism of polymerization was the only photocured mechanism because according to the DSC results, thermal cured happened in the temperature range of 110–200°C.

The thermal properties of the liquid resin and samples considering the different post-curing conditions were analyzed by DSC. According to the results, by the following equation, the cure degree of the samples which

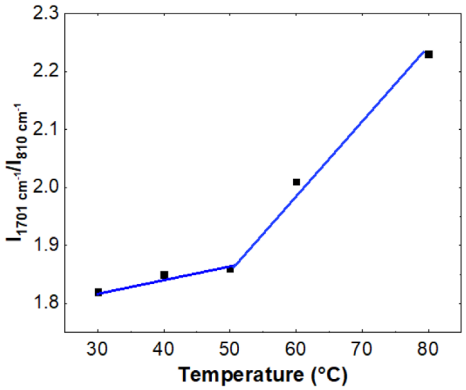

FIGURE 3 The obtained I_{1701}/I_{810} cm^{-1} ratio of absorption from FTIR for post-cured samples in the temperature range of 30–80°C. FTIR, Fourier-transform infrared spectroscopy [Color figure can be viewed at wileyonlinelibrary.com]

indicates the polymerization of the samples after post-curing were investigated[10]:

$$\text{Degree of cure}\,(\%) = \left(1 - \Delta H_{\text{sample}}/\Delta H_{\text{resin}}\right) \times 100, \quad (1)$$

where ΔH_{sample} and ΔH_{resin} are the heat release energy from samples and resin, respectively. Figure 4 shows the heat flow against the temperature for resin. For measuring the ΔH_{resin}, the heat flow from the liquid resin was analyzed and heat release energy was measured equal to 99.34 J/g.

The obtained results of DSC for the green and post-cured samples are indicated in Figure 5. All obtained DSC heating plots show endothermic peaks corresponding to glass transition and one exothermic peak corresponding to thermal curing. According to this

figure, curing was performed in the range of 110–200°C. The maximum and minimum enthalpy were 11.87 and 2.51 J/g which related to the sample without post-curing and post cured sample by UV with the heat presence of 80°C, respectively.

According to the cure degree results, the green sample was 88% cured whereas post-curing by using the light and in the 80°C increase the degree of cure the samples up to 98%. By results, increasing the temperature from 40 to 80°C leads to the increasing the polymerization during the post-curing, which can be attributed to the increasing the mobility of the polymer chain by increasing the temperature. Thus, increasing the temperature leads to the increasing in the chain mobility, and by increasing the polymer network mobility, chain transfer reaction will be increases.[40,41]

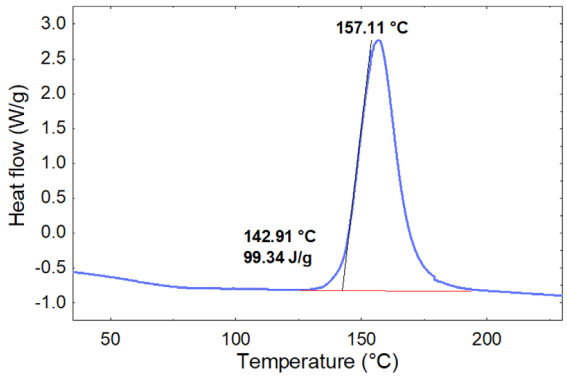

FIGURE 4 The DSC heat flow plot for liquid resin. DSC, differential scanning calorimetry [Color figure can be viewed at wileyonlinelibrary.com]

3.2 | TGA analysis

To investigate the thermal stability of samples TGA was performed. Figure 6 shows the TGA analysis for resin, green and post-cured samples. Figure 6b shows derivative thermogravimetric curves for each sample. According to the results, higher thermal stability of crosslinked polymers compared to the net one was shown which is good agreement with literature.[42]

The results showed a different number of decomposition stage for resin compared to the green and post-cured samples. Loss weight for the resin showed a 2-stages decomposition whereas in other samples was happen in three-stages. The stages of resin decomposition were accrued in 102.9, 352.9, and 438.20°C, which in each steps resin lost were 23.4%, 44.2%, and 34.2%, respectively. First decomposition step is related to the evaporation of volatile components acrylate groups at 102.9°C. Second and third step of the resin degradation were coincided in temperature of first and second degradation stag of green and post-cured samples. As mentioned, in general, all the resin, which used in SLA method can be cured by heating in the certain range. Therefore, resin will be cured by increasing the temperature during the TGA analysis that can be led to the approximately same decomposition temperature compared to the other samples.

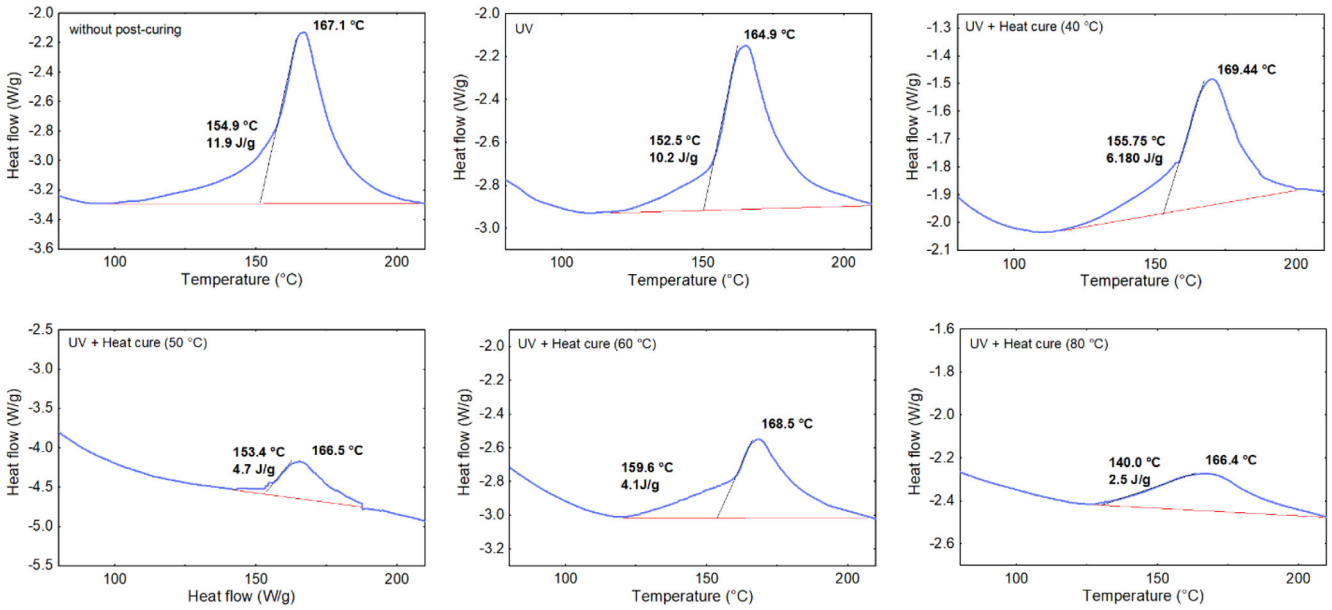

FIGURE 5 The results of DSC for the samples. DSC, differential scanning calorimetry [Color figure can be viewed at wileyonlinelibrary.com]

Green sample and post-cured samples showed more thermal resistance compared to the resin, which represents the important role of cross-links on thermal behavior. The first weight loss in the samples was at 352.9°C, which was accompanied by 52.5% weight loss. This weight loss can be attributed to the trapped volatile materials that are released. The next step happened at 438.20°C that represented completion decrosslinking and thermal degradation. The weight loss of this step was 47.5% and this reduction can be attributed to the decomposition of aromatic structures.[35,37] TRT 80°C showed the best thermal behavior among the other samples, which is related to the density of cross-links in these samples compare to the others.

3.3 | DMTA analysis

DMTA in flexion mode was used to investigate the thermo-mechanical behavior of fabricated samples. Green and post cured 0°-printed samples were selected for this purpose. Figure 7 shows the storage modulus and tan δ for without post cured samples in different frequencies of 1, 3, and 10 Hz. According to Figure 7a, a shift toward a higher temperature of the peak of tan δ was observed by increasing the frequency. Tan δ value is attributed to the phase displacement of the sinusoidal movement of the clamps compared to the responded movement of the samples.[43] The maximum of this displacement which is displayed as a peak can be seen near the Tg caused by the segmental movement of polymer

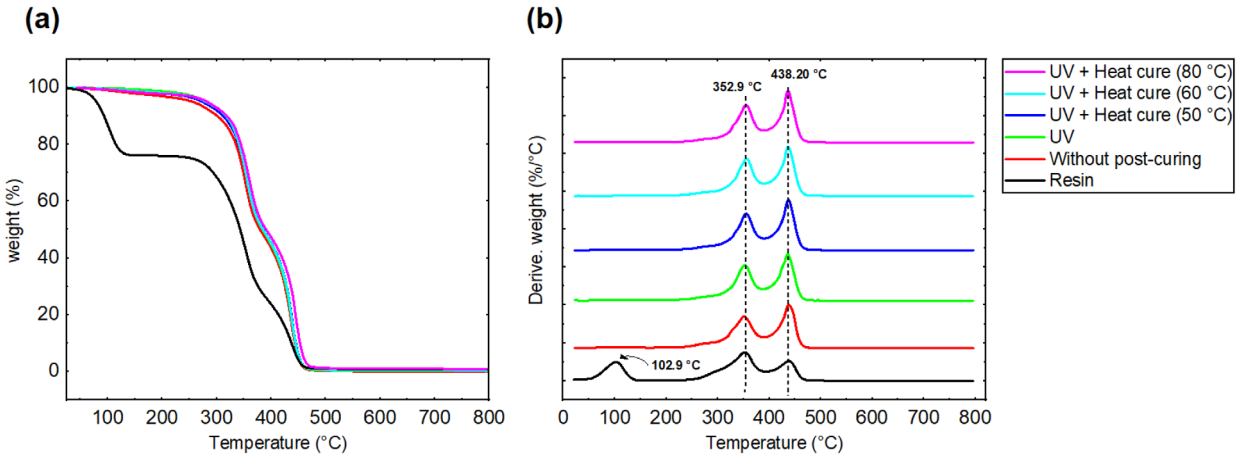

FIGURE 6 Thermal stability of resin, without post cure and post cured: (a) thermogravimetry weight loss and (b) derivative thermogravimetric curve [Color figure can be viewed at wileyonlinelibrary.com]

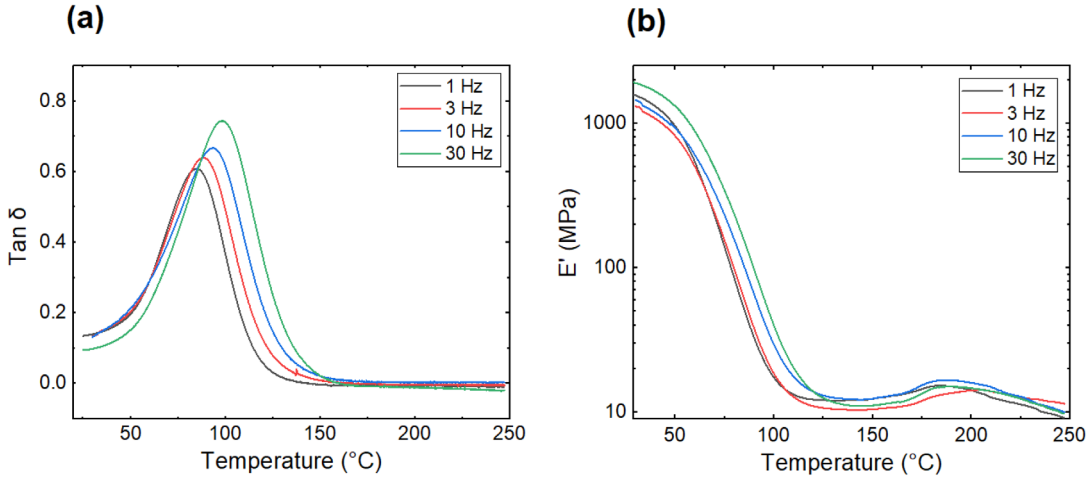

FIGURE 7 (a) Flexion storage modulus (E') and (b) tan δ for green parts in frequencies of 1, 3, 10, and 30 Hz [Color figure can be viewed at wileyonlinelibrary.com]

chains.[44] Increasing the frequency during the test is accompanied by decreasing the segmental molecular motions.[45] So, the segmental motions which have an important role in changing the transition from glassy to the rubbery state become restricted and cause to increasing the Tg.[46] Figure 7b shows the storage modulus against the temperature for different frequencies. Decreasing in E′ was observed by Increasing the temperature up to 150°C which is related to the increasing the mobility of polymeric segments during heating. In the range of 150–250°C modulus was increased and then was reduced again. In this range of temperature residual resins can be cured and subsequently modulus will be increases and again by increasing the temperature E′ was reduced.

Figure 8 shows the storage modulus and tan δ for post-cured samples in frequency of 10 Hz. According to the results of Figure 8a, the lowest Tg was related to the UV-cured sample and then in the other samples, the Tg was increased with increasing the curing temperature that the highest Tg was for heat curing at 80°C with UV. Considering the critical role of segmental motions on Tg and reducing these motions by increasing the polymerization, increasing the glass transition is directly related to the polymerization of parts during post-treatment. According to the Figure 8b, storage modulus at room temperature for UV and UV + heat curing 80°C showed the lowest and highest with 1795.9 and 2307.7 MPa, respectively. All the samples showed a reduces in modulus with increasing the temperature which this reduce was performed by lower rate for UV + Heat cure 80°C compare another. Also, changing in the modulus from 150 up to 210°C show the incomplete cured in the samples and in this range of temperature residual resin were cured. Glass transition of samples is presented in Table 1.

3.4 | Effect of post-curing on mechanical properties

The mechanical properties of green and post cured samples were analyzed for the different sub-build orientations. The maximum tensile strength and elongation results were considered for competing for the mechanical properties of the samples. Figure 9a,b show the stress–strain curve for different orientation printed samples for without and post cured at 80°C, respectively. According to the Figure 9a maximum tensile stress of without post-cured samples for 0°, 45°, and 90° were 25, 20, and 40 MPa, respectively. Also, the maximum strain was for 90°, 45°, and then 0°. Figure 9b shows the stress against the strain for UV + heat cure 80°C for different orientations printed samples. The maximum of stress at break was 55, 44, and 50 MPa for 0°, 45°, and 90°, respectively. In addition, 45°-printed part showed a higher strain at break compared to the 0° and 45°-printed parts.

Figure 10a,b shows micrographs of the fracture surface of 90° printed sample that post-cured at 60°C with respect to the different magnifications after tensile test. Plastic deformation area along with other region of brittle failure can be observed in fractured surface of Figure 10a. The plastic deformation region can be attributed to the chain slippage which flaw propagation speed is reduced by the stress release. In addition, fractured surface of Figure 10b shows a region with the layer forms that can be indicated the layered nature of parts printed by this method. In other regions of this figure, the failure is not

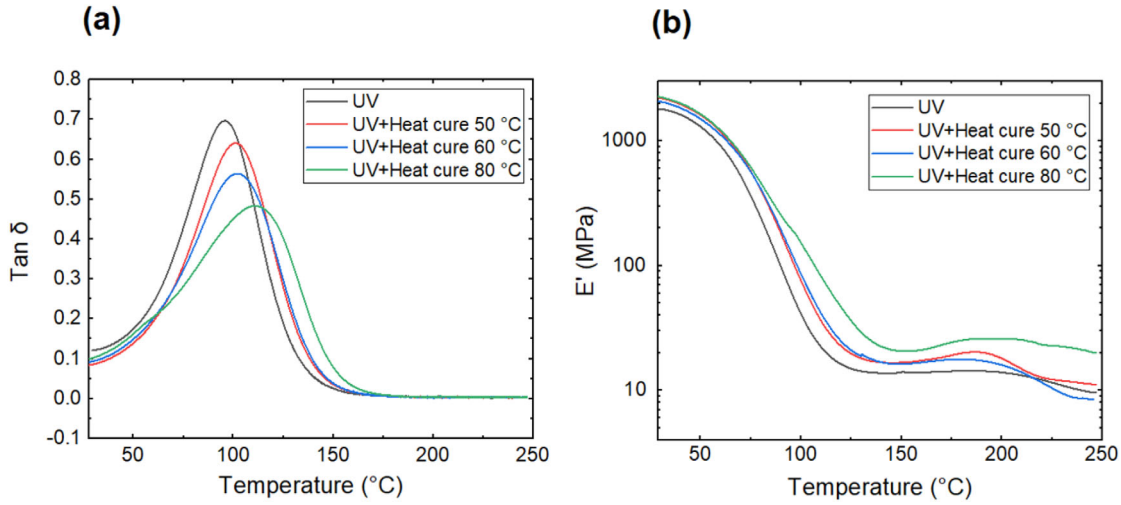

FIGURE 8 (a) Flexion storage modulus (E') and (b) tan δ for post-cured samples in frequencies 10 Hz [Color figure can be viewed at wileyonlinelibrary.com]

observed layer by layer which seems to the fact that the curing has been done completely in this area.[8]

Figure 11a,b are shown the maximum tensile strength and % elongation, respectively. The results showed a significant effect of post-curing on the tensile strength and % elongation of samples. In general, post-curing led to a decrease in the % elongation of the samples. Increases in the maximum tensile strength of the samples by post-curing can be referred directly to the amount of polymerization of samples. It should be mentioned that uncured resin, which is between the layers, or the surface of the parts known as a place with poor mechanical properties, which leads to a reduction in the mechanical properties of the part.[1,14,47] Therefore, improvement of the mechanical properties can be expected by increasing the amount of polymerization in the samples. In addition, in a study by Salmoria et al.[8] the release of internal stress concentration in the samples during the post-curing as one of the important factors to improving the mechanical

TABLE 1 Tg value of samples identified as a peak of tan δ

Sample name	Frequency (Hz)	Tg (°C)
Without post-curing	1	85.4
Without post-curing	3	89.0
Without post-curing	10	94.46
Without post-curing	30	99.19
UV	10	96.59
UV + heat cure 50°C	10	102.34
UV + heat cure 60°C	10	104.34
UV + heat cure 80°C	10	113.99

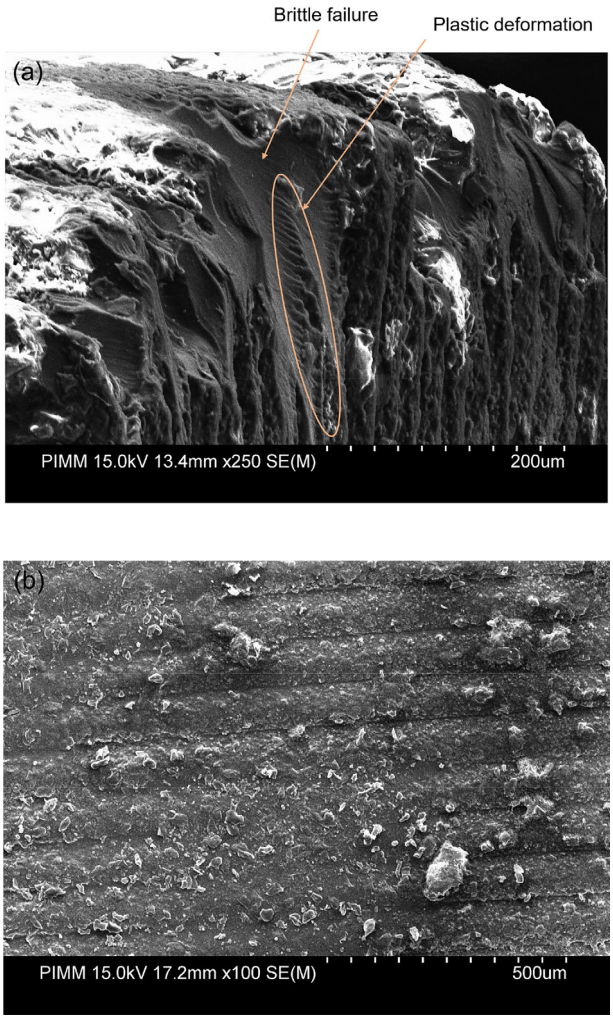

FIGURE 10 Fracture surface of 0° printed sample and post-cured at 60°C with respect to the (a) more magnification and (b) lower magnification [Color figure can be viewed at wileyonlinelibrary.com]

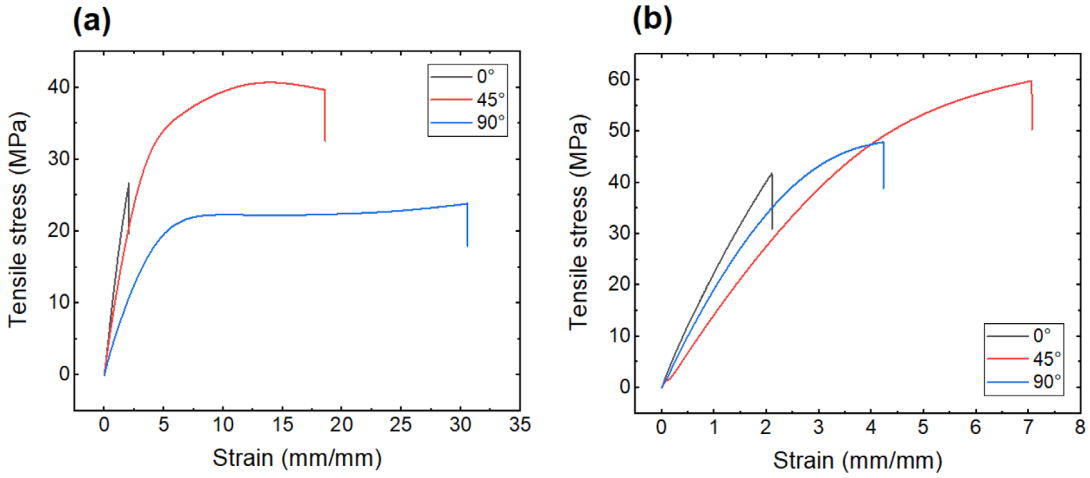

FIGURE 9 Stress–strain curve of samples in different print orientation: (a) without post curing and (b) post-cured at 80°C [Color figure can be viewed at wileyonlinelibrary.com]

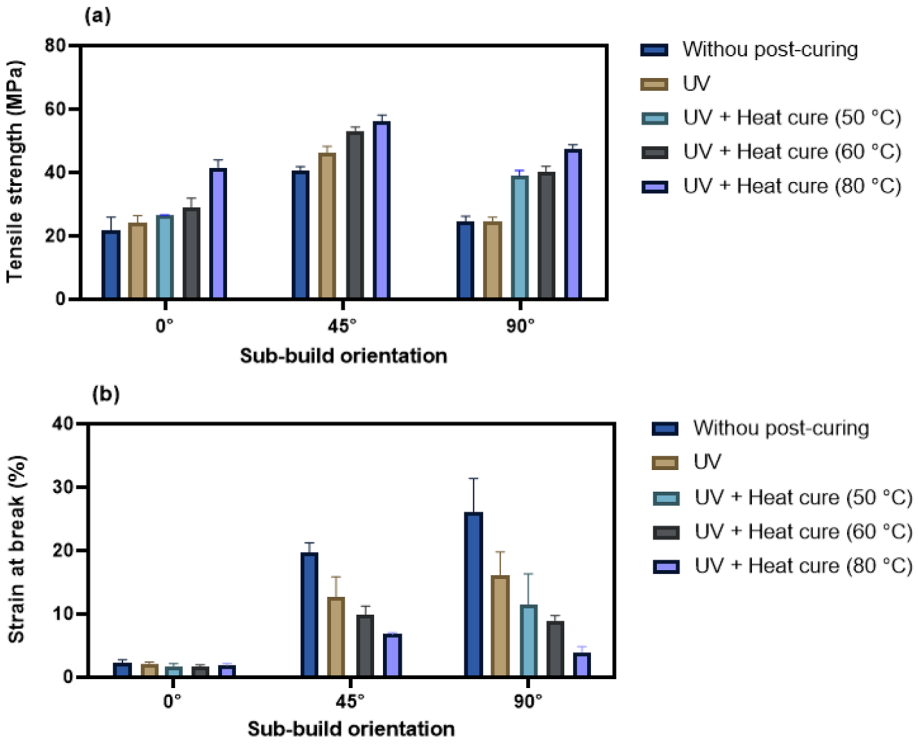

FIGURE 11 (a) Maximum tensile strength and (b) % elongation for green and post-cured samples [Color figure can be viewed at wileyonlinelibrary.com]

properties have been considered. Therefore, polymerization and release of the internal stress can well explain the increase in mechanical properties by increasing the temperature in the post curing for the samples.

As mentioned, the mechanical properties of the fabricated parts were also examined in different sub-build orientations. According to the results, the maximum tensile strength can be ranked as follows: 90° < 0° < 45°. So that the samples without heat treatment showed 0°, 45°, and 90° maximum elongation were equal to 2.83%, 12.37%, and 30.96%, respectively. According to the results, the maximum tensile strength was achieved for the orientation of 45°. It is related to the angle of the layers is at an angle to the force direction. Also, according to Saini et al.[48] it was shown that the elastic modulus of the samples printed by the SLA method at an angle of 45° showed a higher elastic modulus than the sample of other printed angles which is referred to the elastic properties in this orientation.

As can be seen from the results the maximum tensile strength was reduced by increasing the angle orientation from 45° to 90°. On the other hand, by increasing the angle orientation from 45° to 90°, % elongation was increased. Microstructure of the fabricated parts by SLA can be divided into three regions: over-cured resin, cured resin, and non-cured resin. The region of the non-cured resin is between the layers or on the surface of the samples.[1,14] In a study by Asmussen et al.[49] they introduced the non-reacted monomer as a plasticizing parameter on the polymer which can impact the physical and mechanical properties. Given that the 90° and 45° samples were tensioned in the direction of the layers it can seem that the plasticizing effect of residual resin was maximum. However, due to the angle of the layers with the direction of tension, this effect can be insignificant for the angle of 0°.

4 | CONCLUSION

In this study, the effect of post-curing at different temperature ranges in a certain time on the mechanical properties for UDMA resin was investigated. The mechanical properties of green and post cured samples were analyzed for the different sub-build orientations. Physico–chemical, thermal and mechanical properties were investigated by DSC, FTIR, TGA, DMA, and tensile analysis. The obtained result explained the curing mechanism of the samples in the post-curing and the value of residual resin was calculated. Key role of residual resin in the parts on thermal and mechanical analysis was explained. This effect was investigated on the glass transitions of the samples, so that post curing caused to the increasing the glass transition. According to the results, an increase in the post-curing temperature process increased the tensile strength so that the post-curing at 80°C caused to the increasing the polymerization up to 98%. Finally, results showed the maximum of tensile strength in the rank of 90° < 0° < 45°.

ACKNOWLEDGMENT

The authors thankfully acknowledge of ADEME support (ECOLOCAR project).

AUTHOR CONTRIBUTIONS

Nader Zirak: Conceptualization (lead); data curation (lead); formal analysis (lead); investigation (lead); writing – original draft (lead). **Mohammadali Shirinbayan:** Conceptualization (lead); methodology (lead); validation (lead); writing – review and editing (lead). **Khaled Benfriha:** Methodology (lead); writing – review and editing (lead). **Michael Deligant:** Conceptualization (lead); investigation (lead); writing – review and editing (lead). **Abbas Tcharkhtchi:** Conceptualization (lead); supervision (lead); writing – review and editing (lead).

DATA AVAILABILITY STATEMENT

The data that support the findings of this study are available from the corresponding author upon reasonable request.

ORCID

Nader Zirak https://orcid.org/0000-0001-8551-6943

REFERENCES

[1] J. R. C. Dizon, A. H. Espera Jr.., Q. Chen, R. C. Advincula, *Addit. Manuf.* **2018**, *20*, 44.
[2] N. Zirak, M. Shirinbayan, M. Deligant, A. Tcharkhtchi, *Polymers* **2022**, *14*, 97.
[3] A. Milovanović, M. Milošević, G. Mladenović, B. Likozar, K. Čolić, N. Mitrović, *Exp. Num Invest. Mater. Sci. Eng.* **2018**, *54*, 84.
[4] D. N. Lastovickova, F. R. Toulan, J. R. Mitchell, D. VanOosten, A. M. Clay, J. F. Stanzione III., G. R. Palmese, J. J. la Scala, *J. Appl. Polym. Sci.* **2021**, *138*, app50574.
[5] X. Zhang, Y. Xu, L. Li, B. Yan, J. Bao, A. Zhang, *J. Appl. Polym. Sci.* **2019**, *136*, 47487.
[6] J. Z. Manapat, Q. Chen, P. Ye, R. C. Advincula, *Macromol. Mater. Eng.* **2017**, *302*, 1600553.
[7] M. Danish, P. Vijay Anirudh, C. Karunakaran, V. Rajamohan, A. T. Mathew, K. Koziol, V. K. Thakur, C. Kannan, A. S. S. Balan, *J. Appl. Polym. Sci.* **2021**, *138*, 50903.
[8] G. V. Salmoria, C. H. Ahrens, M. Fredel, V. Soldi, A. T. N. Pires, *Polym. Test.* **2005**, *24*, 157.
[9] G. Rosace, R. Palucci Rosa, R. Arrigo, G. Malucelli, *J. Appl. Polym. Sci.* **2021**, *138*, 51292.
[10] J. Y. H. Fuh, L. Lu, C. C. Tan, Z. X. Shen, S. Chew, *J. Mater. Process Technol.* **1999**, *89*, 211.
[11] C. Decker, *Nucl. Instruments Methods Phys. Res. Sect. B Beam Interact. Mater. Atoms* **1999**, *151*, 22.
[12] A. Bagheri, J. Jin, *ACS Appl. Polym. Mater.* **2019**, *1*, 593.
[13] N. Abbasnezhad, N. Zirak, M. Shirinbayan, S. Kouidri, E. Salahinejad, A. Tcharkhtchi, F. Bakir, *J. Appl. Polym. Sci.* **2021**, *138*, 50083.
[14] G. V. Salmoria, C. H. Ahrens, V. E. Beal, A. T. N. Pires, V. Soldi, *Mater Des.* **2009**, *30*, 758.
[15] Y. Deng, J. Li, Z. He, J. Hong, J. Bao, *J. Appl. Polym. Sci.* **2020**, *137*, 49294.
[16] C. M. Cheah, A. Y. C. Nee, J. Y. H. Fuh, L. Lu, Y. S. Choo, T. Miyazawa, *J. Mater. Process Technol.* **1997**, *67*, 41.
[17] J. Martín-Montal, J. Pernas-Sánchez, D. Varas, *Polymers* **2021**, *13*, 1147.
[18] T. Gebäck, A. Heintz, *A Pore Scale Model for Osmotic Flow: Homogenization and Lattice Boltzmann Simulations. Transp Porous Media*, Vol. 126, Springer, Netherlands **2019**, p. 161.
[19] R. Hague, S. Mansour, N. Saleh, R. Harris, *J. Mater. Sci.* **2004**, *39*, 2457.
[20] D. S. Kumar, M. J. Shukla, K. K. Mahato, D. K. Rathore, R. K. Prusty, B. C. Ray, *IOP Conf. Ser. Mater. Sci. Eng.* **2015**, *75*, 12012.
[21] A. C. Uzcategui, A. Muralidharan, V. L. Ferguson, S. J. Bryant, R. R. McLeod, *Adv. Eng. Mater.* **2018**, *20*, 1800876.
[22] N. Chantarapanich, P. Puttawibul, K. Sitthiseripratip, S. Sucharitpwatskul, S. Chantaweroad, *Songklanakarin J. Sci. Technol.* **2013**, *35*, 91.
[23] C. Mendes-Felipe, D. Patrocinio, J. M. Laza, L. Ruiz-Rubio, J. L. Vilas-Vilela, *Polym. Test.* **2018**, *72*, 115.
[24] J. Zhao, Y. Yang, L. Li, *J. Manuf. Process.* **2020**, *56*, 867.
[25] Y. Yang, L. Li, J. Zhao, *Mater. Des.* **2019**, *162*, 418.
[26] R. Gauvin, Y.-C. Chen, J. W. Lee, P. Soman, P. Zorlutuna, J. W. Nichol, H. Bae, S. Chen, A. Khademhosseini, *Biomaterials* **2012**, *33*, 3824.
[27] B. Wang, G. Ding, K. Chen, S. Jia, J. Wei, Y. Wang, R. He, Z. Shao, *J. Appl. Polym. Sci.* **2020**, *137*, 49164.
[28] A. Chiappone, F. Bella, J. R. Nair, G. Meligrana, R. Bongiovanni, C. Gerbaldi, *ChemElectroChem* **2014**, *1*, 1350.
[29] L. Novakova-Marcincinova, J. Novak-Marcincin, *Proc Manuf Syst.* **2013**, *8*, 87.
[30] Q. Alsandi, M. Ikeda, Y. Arisaka, T. Nikaido, Y. Tsuchida, A. Sadr, N. Yui, J. Tagami, *Sensors* **2021**, *21*, 3331.
[31] T. Zhao, R. Yu, X. Li, Y. Zhang, X. Yang, X. Zhao, W. Huang, *J. Mater. Sci.* **2019**, *54*, 5101.
[32] T. Buruiana, V. Melinte, L. Stroea, E. C. Buruiana, *Polym. J.* **2009**, *41*, 978.
[33] F. L. B. Amaral, V. Colucci, R. G. Palma-Dibb, C. SAM, *J. Esthet. Restor. Dent.* **2007**, *19*, 340.
[34] O. Konuray, J. M. Salla, J. M. Morancho, X. Fernández-Francos, M. García-Alvarez, X. Ramis, *Thermochim. Acta.* **2020**, *692*, 178754.
[35] A. Barkane, O. Platnieks, M. Jurinovs, S. Gaidukovs, *Polym. Degrad. Stab.* **2020**, *181*, 109347.
[36] S. Gaidukovs, A. Medvids, P. Onufrijevs, L. Grase, *Express Polym. Lett.* **2018**, *12*, 918.
[37] D. Kunwong, N. Sumanochitraporn, S. Kaewpirom, *Sonklanakarin J. Sci. Technol.* **2011**, *33*, 201.
[38] Z. Li, X. Yang, L. Wu, Z. Chen, Y. Lin, K. Xu, G. Q. Chen, *J. Biomater. Sci. Polym. Ed.* **2009**, *20*, 1179.
[39] H. Pelletier, N. Belgacem, A. Gandini, *J. Appl. Polym. Sci.* **2006**, *99*, 3218.
[40] C. Dall'Argine, A. Hochwallner, N. Klikovits, R. Liska, J. Stampf, M. Sangermano, *Macromol. Mater. Eng.* **2020**, *305*, 2000325.
[41] Z. Yang, G. Wu, S. Wang, M. Xu, X. Feng, *J. Polym. Sci. Part B Polym. Phys.* **2018**, *56*, 935.
[42] M. Lebedevaite, J. Ostrauskaite, E. Skliutas, M. Malinauskas, *Polymers* **2019**, *11*, 116.
[43] A. Ji, S. Zhang, S. Bhagia, C. G. Yoo, A. J. Ragauskas, *RSC Adv. Royal Soc. Chem.* **2020**, *10*, 21698.
[44] R. P. White, J. E. G. Lipson, *Macromolecules* **2016**, *49*, 3987.

[45] G. Li, P. Lee-Sullivan, R. Thring, *J. Therm. Anal. Calorim.* **2000**, *60*, 377.
[46] Bird D, Caravaca E, Laquidara J, Luhmann K, Ravindra NM. Formulation of Curable Resins Utilized in Stereolithography. TMS 2019 148th Annual Meeting and Exhibition Supplemental Proceedings; **2019**. p. 1575–87.
[47] Z. Weng, Y. Zhou, W. Lin, T. Senthil, L. Wu, *Compos. Part A Appl. Sci. Manuf.* **2016**, *88*, 234.
[48] J. S. Saini, L. Dowling, J. Kennedy, D. Trimble, *Proc. Instit. Mech. Eng. Part C J. Mech. Eng. Sci.* **2020**, *234*, 2279.
[49] S. V. Asmussen, G. F. Arenas, C. I. Vallo, *Prog. Org. Coat.* **2015**, *88*, 220.